iJRASET
International Journal For Research in Applied Science and Engineering Technology

INTERNATIONAL JOURNAL FOR RESEARCH

IN APPLIED SCIENCE & ENGINEERING TECHNOLOGY

Volume: 9 **Issue:** X **Month of publication:** October 2021

DOI: https://doi.org/10.22214/ijraset.2021.38579

www.ijraset.com

Call: 08813907089 | E-mail ID: ijraset@gmail.com

International Journal for Research in Applied Science & Engineering Technology (IJRASET)
ISSN: 2321-9653; IC Value: 45.98; SJ Impact Factor: 7.429
Volume 9 Issue X Oct 2021- Available at www.ijraset.com

Regional Climate Modelling using Advanced Research WRF for simulation of long term rainfall in Uttarakhand Himalaya in CORDEX framework

Tanmay Dhar[1], Mario M. Miglietta[2], Bhupendra S. Rawat[3]
[1, 3]*Department of Physics, Uttaranchal University, Dehradun 248007, India*
[2]*National Research Council of Italy—Institute of Atmospheric Sciences and Climate (CNR-ISAC), 35127 Padua, Italy*

***Abstract:** With the most fragile and complex environment having rich repository of biodiversity and water, the terrains of Uttarakhand Himalaya is always challenging for regional climate modelling. In this work, three different versions of land surface schemes are used to simulate the climate over this complex terrain for the period of 1995-2010 with a horizontal resolution of 0.44^0, using the Advanced Weather Research and Forecasting (WRF-ARW) model.*

I. INTRODUCTION

The study area, Garhwal Himalaya is located from 30^0 N to 31^0 N latitude and 70^0 E to 78^0 E longitudes and comprises 32450 km^2 area (Figure 1). Garhwal Himalaya region is located in the Indian Himalayan monsoonal subcontinent and mainly three seasons are present in a year: warm summer (March to June), humid warm summer (July to June), winter season (November to February). The climatic conditions of the Garhwal Himalayan region vary from the tropical to glacial cover zone. On the basis of temperature, precipitation and altitude Garhwal Himalaya divided into seven different climatic zones from south to north: tropical (< 300 m), subtropical (301-800 m), warm temperate (801-1600 m), cool temperate (1601-2400 m), cold temperate (2401-3200 m), sub-alpine (3201-4000), and glacial cover (> 4000 m) (Kaushik, S.D., 1962).

The elevation ranges from 474m (Devaprayag) to 3892m (Gomukh glacier, CWC, 2020). Total number of glaciers identified in Ganga basin is 968 with the glacier covered area coming to about 2,850 km^2, which is less than 8% of the total basin area. Largest number of glaciers- totaling 407- has been identified in the Alaknanda basin that occupies 1,230 km^2, which accounts for almost 11% of total basin area (Glacier Atlas of India, GSI, 2017). The land under agriculture is 644.22 km^2, which is 5.9 percent of the total geographical area while only 64.8 km^2 (0.6%) land is under the horticultural crops (Sati VP, 2008). Around 60% of the basin is under the agrarian activity (main crop assortments that incorporate wheat, maize, rice, sugarcane, bajra and potato), while 20% is roofed by backwoods, generally inside the higher mountains, roughly 2% in the mountain peaks is permanently covered with the snow. The annual normal precipitation inside this basin ranges between 550 and 2500 mm (Shukla et al., 2014), and a significant part of the precipitation is contributed by the south-westerly monsoon that prevails from July to late September. The geographical location and elective subtleties of the study region of Alakananda and Bhagirathi basin are given in Figure 1.

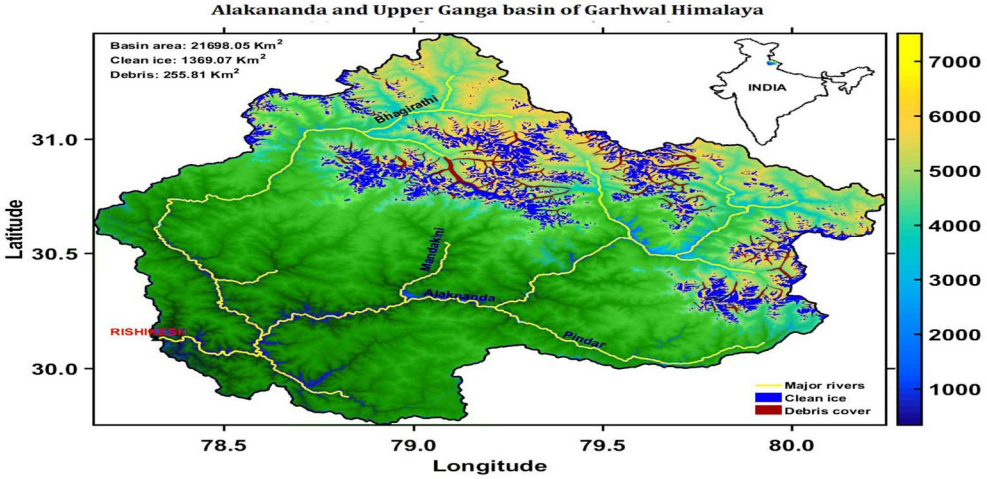

Figure 1. Elevation of Garhwal Himalyas

II. MODEL AND DATA

The simulations with the most advanced framework of WRF model (version 3.7.1) (Skamarock et al. 2008) with horizontal resolution of 0.44° (≈ 50 km) and 18 vertical levels, following the guidelines of CORDEX (Giorgi et al. 2009), have been applied to resolve the influence of the most sensitive land surface processes in the simulation of mean climate over the topographically complex region of Uttarakhand Himalaya. The Weather Research and Forecasting (WRF) model is a community nonhydrostatic and fully compressible atmospheric model, maintained by the National Center for Atmospheric Research (NCAR). The model setup used here includes the Yonsei University (YSU) Planetary Boundary Layer scheme, the Kain–Fritsch (KF)cumulus scheme, the WSM6 cloud microphysics scheme and RRTMG scheme for long- and short- wave radiation parameterizations. This configuration remains unchanged for all three simulations performed for this study, and the only component of the configuration that is altered is the land surface scheme (LSS). The three different LSSs used here are Noah-MPMP (multi-physics) (Niu 2011), Community Land Model (CLM) (CGD 2010) and the Rapid Update Cycle (RUC) (Benjamin et al. 2004).

The main features of the three LSSs, which differ in the complexity of the treatment of the land surface and associated processes (Table 1), are utilised in three simulations driven by the ERA-Interim re-analyses.

For the simulation, the model requires time-dependent lateral (vertical profiles of wind, temperature and humidity) and surface (surface pressure and sea surface temperature) boundary conditions updated with an interval of 6 hours. The land surface models available with the WRF package are described in the following:

A. Noah- Multiphysics (Noah-MP)

The Noah-MP land surface model (LSM) is one of the most robust and well-established models of its kind for meteorological and climate modeling with multiple options for key land-atmosphere interaction processes (Niu et al., 2011). Noah-MP contains a separate vegetation canopy defined by a canopy top and bottom, crown radius, and leaves with prescribed dimensions, orientation, density, and radiometric properties. The canopy employs a two-stream radiation transfer approach along with shading effects necessary to achieve proper surface energy and water transfer processes including under-canopy snow processes (Dickinson, 1983; Niu and Yang, 2004). Noah-MP contains a multi-layer snowpack with liquid water storage and melt/refreeze capability and a snow-interception model describing loading/unloading, melt/refreeze capability, and sublimation of canopy-intercepted snow (Yang and Niu 2003; Niu and Yang 2004). Multiple options are available for surface water infiltration and runoff and groundwater transfer and storage including water table depth to an unconfined aquifer (Niu et al., 2007). The Noah-MP model can be executed by prescribing both the horizontal and vertical density of vegetation using either ground- or satellite-based observations. Another available option is for prognostic vegetation growth that combines a Ball-Berry photosynthesis-based stomatal resistance (Ball et al., 1987) with a dynamic vegetation model (Dickinson et al. 1998) that allocates carbon to various parts of vegetation (leaf, stem, wood and root) and soil carbon pools (fast and slow). The model is capable of distinguishing between C3 and C4 photosynthesis pathways and defines vegetation-specific parameters for plant photosynthesis and respiration.

B. Rapid Update Cycle (RUC)

The RUC LSM became operational at the NOAA/National Centers for Environmental Prediction (NCEP) first, as part of the RUC from 1998–2012, and then as part of the Rapid Refresh Model (RR or RAP) from 2012 through the present and as part of High Resolution Rapid Refresh (HRRR)from 2014 through the present. The simple treatments of basic land surface processes in the RUC LSM (Smirnova et al. 2016) have proven to be physically robust and capable of realistically representing the evolution of soil moisture, soil temperature, and snow in cycled models. Extension of the RAP domain to encompass all of North America and adjacent high-latitude ocean areas necessitated further development of the RUC LSM for application in the tundra permafrost regions and over Arctic sea ice (Smirnova et al. 2000). Other modifications include refinements in the snow model and a more accurate specification of albedo, roughness length, and other surface properties. These recent modifications in the RUC LSM are described and evaluated in Smirnova et al. 2016.

The parameterizations in the RUC LSM describe complicated atmosphere–land surface interactions in an intentionally simplified fashion to avoid excessive sensitivity to multiple uncertain surface parameters. Nevertheless, the RUC LSM, when coupled with the hourly-assimilating atmospheric model, demonstrated over years of ongoing cycling (Benjamin et al. 2004a,b ; Berbery et al. 1999) that it can produce a realistic evolution of hydrologic and time-varying soil fields (i.e., soil moisture and temperature) that cannot be directly observed over large areas, as well as the evolution of snow cover on the ground surface. This result is possible only if the soil–vegetation–snow component of the coupled model, constrained only by atmospheric boundary conditions and the specification of surface characteristics, has sufficient skill to avoid long-term drift.

C. Community Land Model (CLM)

CLM is a land surface model developed at National Centre for Atmospheric Research and already integrated to Community Climate System Model (CCSM). The CLM represents several aspects of the land surface including surface heterogeneity and consists of submodels related to land biogeophysics, the hydrological cycle, biogeochemistry, and ecosystem dynamics. The software system of the global offline CLM includes physical earth system components, such as the CLM, data atmosphere (a proxy atmosphere model, which reads in atmospheric forcings to drive the CLM), stub ocean, stub ice and stub glacier. It contains an application driver to configure the parallel computing environment and the whole simulation system (physical earth system components and flux coupler between those components). CLM incorporates five diverse snow layers with representation of trace snow. It has higher number of soil layers and includes 10 unevenly spaced soil layers up to the depth of 3m. The equation for the calculation of temperature, liquid water and ice content is solved for each characterized layer in this model. For portrayal of the surface heterogeneity, a mosaic-tile type approach is accomplished. For this, a single model grid cell can be split to four distinct classes of land use in particular vegetation, wetland, glacial mass and lake. Once more, the vegetated region itself can be isolated into 17 diverse plant function types (PFTs). The surface hydrology and energy balance conditions are solved for each class inside a model framework and returned back to the coarser grid subsequent to averaging. WRF has a choice of utilizing the portrayal of land-surface processes as Community Land Model (Oleson et al., 2008). Previously, the land surface model was initialized with constant soil moisture for different regions of the globe while now it is initialized with the climatologically available soil moisture values thereby reducing the spin up periods especially for deeper soil layers.

III. EXPERIMENTAL DESIGN

A suit of three continuous model integrations have been carried out for the period 1995-2010 starting from 01 January and terminating on 31st December. The recent version of WRF (version 3.7.1) has been used for the downscaling experiment over the COordinated Regional Climate Downscaling EXperiment – South Asia (CORDEX-SA) domain. The region extends between 10-130°E in longitude and -22°S-50°N in longitude and covers most of the parts of South Asian region. The model integration has been carried out a grid spacing of 50km with 18 vertical levels while model top is prescribed as 50hPa. For driving the regional model, prognostic variables (u, v, t, q, ps) along with the sea surface temperature has been obtained from the CMIP6 (Coupled Model Inter-comparison Project phase 6) programme of World Climate Research Programme (WCRP). The selection of input forcing has been carried out in a separate exercise based on the review of available literature. The Global Climate Models (GCMs) able to represent the Indian Summer Monsoon (ISM, hereafter) and its associated features such as the large-scale flow, mean precipitation climatology, inter-annual and intra-seasonal variability, spatial variability of precipitation, simulation of large scale features have been assessed from different available models over Indian region before finalization of the GCM forcing. In order to analyze the sensitivity of the land surface treatment and its role in representation of the surface hydrology in a regional climate model framework over a topographically heterogeneous region like Himalayas, 3 different available land surface models have been employed as 3 different cases. For simulation of each case, land surface models have been changed and picked from Noah-MP, RUC and CLM4. The other parameterization schemes have been kept constant for each case following the description provided in the table. An initial spin-up period of 5 years has been discarded and the 15 years of period (1995-2010) has been taken for further analysis. The dynamics and hydrostatics of the model configuration has been presented in Table 1. The model topography for each model experiments are shown (Figure 4).

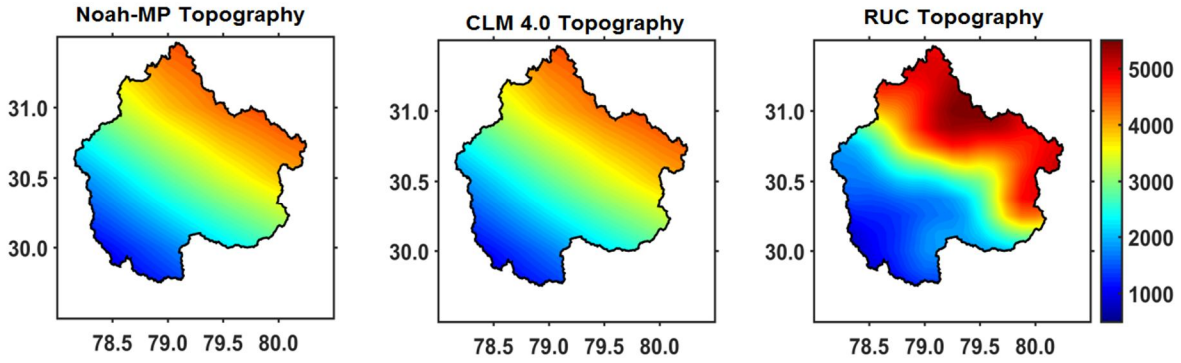

Figure 2. Model simulated topography over the study area from different model experiment

Table 1: Model configuration for the downscaling experiments.

Dynamics	**Hydrostatics**
Model	WRF-3.7.1
Model Domain	CORDEX-SA, 10°E-130°E and 22°S-50°N
Resolution	50 Km horizontal and 18 vertical sigma levels
Initial and boundary conditions	MIROC6 from CMIP6 programme Prognostic Variables (u, v, t, q, ps)
SST	MIROC6
Land surface treatment	A) Noah-MPMP (NOAH-MP) B) RUC (RUC) C) CLM4 (CLM)
Radiation Parameterization	RRTMG
PBL parameterization	YSU
Cumulus Parameterization	KF
Cloud Microphyics	WSM6
Period	1995-2010

A. Precipitation (mm/day)

This spatial distribution of simulated and observed seasonal daily mean precipitation (mm/day) over Bhagirathi river basin is represented for different experiments during historical period (1995-2010). The different simulations vary from each other in the representation of Land surface parameterisation: Noah-MP, CLM4 and RUC. The simulated rainfall has been compared against the corresponding APHRODITE (Yatagai et al., 2012) data set at 50-km horizontal resolution (Figure 5) for all the four meteorological season such as pre-monsoon (Mar – May: MAM, hereafter), monsoon (Jun – Sep: JJAS, hereafter), post-monsoon (Oct – Dec: OND, hereafter) and winter (Jan – Feb: JF, hereafter).

The observation (APHRODITE) shows highest precipitation during monsoon season. The maximum precipitation is observed in the southern part of the UGB whereas relatively less rainfall occurs in the higher altitudes or northern parts of the domain (Figure 3c). The lowest precipitation is found during post-monsoon and winter (Figure 3d & a); the rainfall during MAM is slightly higher as compared to winter (Figure 3b).

The NOAH-MP simulation shows the highest precipitation during MAM (Figure 3f) and the lowest is observed in OND (Figure 3h). However, the rainfall is much less in NOAH-MP simulation as compared to observation which varies up to 9mm/day. The simulation with CLM as the land-surface treatment has higher rainfall during MAM and JJAS (Figure 3j & 3k), while least rainfall is found during OND (Figure 3l).

The highest rainfall during these seasons ranges from 3-12 mm/day. The JF receives more rainfall as compared to OND (Figure 3i & l) with the highest magnitude of 8mm/day. The seasonal and spatial distribution of rainfall for RUC is similar to CLM (Figure 3i - p) with highest rainfall during MAM and JJAS, while least in OND. The rainfall during MAM and JJAS varies from 3-12 mm/day.

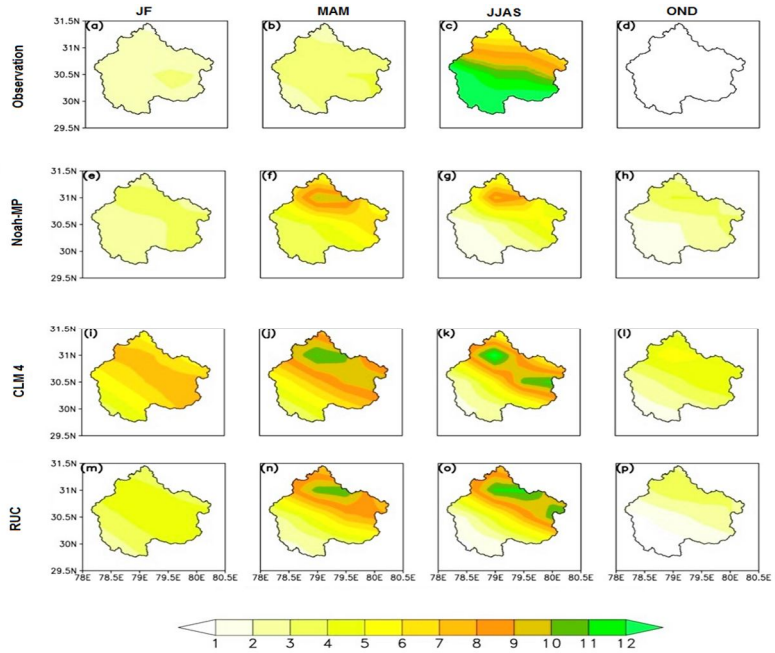

Figure 3. Seasonal daily mean precipitation (mm/day) over Bhagirathi river basin from different experiments during historical period (1995-2010) from WRF 3.7.1 model with observation data.

In the observation, higher precipitation is distinctly found in the monsoon season i.e., JJAS whereas the models show higher precipitation in two seasons, such as MAM and JJAS. The model simulated rainfall for all three experiments during MAM exceeds the observed value. The magnitude of rainfall in NOAH-MP simulation across the Bhagirathi-Alaknanda basin is much less as compared to CLM and RUC for all seasons. The area-averaged magnitude (6.78 mm/d and 6.24 mm/d) of the rainfall during JJAS is closer for CLM and RUC. It is interesting to observe that the simulated rainfall is found to be higher in the higher elevated regions of the UGB, which is completely opposite to the observed value. This behavior of the model may be attributed to the higher moisture availability and improper representation moisture-orography interactions.

B. Precipitation Bias (mm/day)

The models bias, in different experiments, shows almost similar spatial structure for all the seasons (figure 4a-l). The model shows a positive bias for MAM, OND and JF. However, the higher rainfall in the high altitude of the northern basin leads to wet bias whereas relatively lesser rainfall in the plains results in the dry bias over the southern part of the study domain.

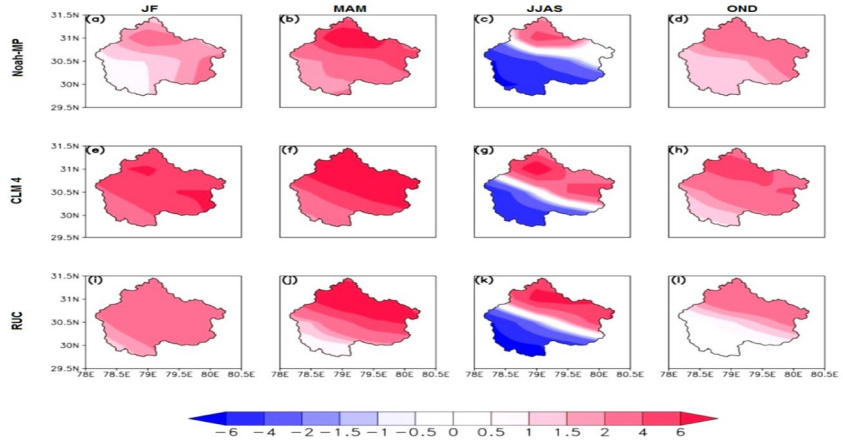

Figure 4. Mean bias of precipitation, calculated as model minus observation (mm/day) from different experiments during historical period (1995-2010) over Bhagirathi-Alaknanda basin for different seasons from WRF 3.7.1 model, is shown in fig (a-l) respectively.

In the NOAH-MP simulation, the seasonal rainfall is generally higher as compared to the observed value except JJAS, but with a drastic underestimation over southern UGB during JJAS. Similar results are also obtained from the analysis of CLM and RUC. Interestingly, a negative precipitation anomaly is found over the southern flank of the basin during OND for RUC (Figure 4l). The overall distributions of biases show that the model simulation has higher precipitation over the upper reaches of GRB, where the altitude is very high, and lower precipitation over the plains of river Ganga, in agreement with a recent study that shows a clear contrasting signal of increasing and decreasing seasonal mean precipitation between upper and lower parts of the basin for all seasons (Nepal & Shrestha, 2015; Panday et al., 2015). The higher precipitation in the higher elevation regions is attributed to the possible increase in temperature. The Moisture-topography-temperature feedback in conjugate manner drives this mechanism. In another studies, wetter cold season over upper GRB is reported (Nepal & Shrestha, 2015; Panday et al., 2015). Distinct decrease of precipitation in lower GRB could be a matter of concern for agriculture, socio-economic aspects and so on.

C. Elevation vs Precipitation

This section examines the elevation-dependency of the precipitation along the Bhagirathi-Alaknanda basin. The simulated as well as the observed rainfalls are interpolated to 1km * 1km grid of GTOPO (Gesch & Greenlee, 1996) over the basin. The height and precipitation are extracted for each grid point and compared to analyse the elevation-dependent rainfall pattern over Bhagirathi-Alaknanda basin (Figure 5). The observed value shows that the rainfall is unaffected by the altitude during MAM, JF and OND. However, the peak rainfall season JJAS shows a decrease of the rainfall with altitude (Figure 5c). Similar analysis for NOAH-MP simulation shows that during MAM and JJAS, the rainfall increases with altitude and the maximum rainfall is found at a height of 4km (Figure 5e-h). At higher elevations, the rainfall decreases with height. The magnitude of rainfall during JF and OND is lesser as compared to the other seasons; however, the pattern is similar with highest rainfall around 4km but not prominent.The simulation with CLM as land surface scheme also follows the same pattern as NOAH-MP, where the maximum rainfall is found at 4km altitude. But, the magnitude of simulated rainfall is higher in CLM for all season. The simulation with RUC features shows some interesting results (Figure 5m-p) as compared to other simulations. The rainfall is found to be increasing with height except for DJF. The highest rainfall is found at an altitude of 6km (4km) for OND, JJAS and MAM (JF). The increase of rainfall with height and further decrease after a certain height indicating a one-way topography (Bookhagen & Burbank, 2010). Therefore, it can be inferred that the NOAH-MP and CLM follows a one-way topography, while RUC shows a monotonous increase of rainfall with altitude.

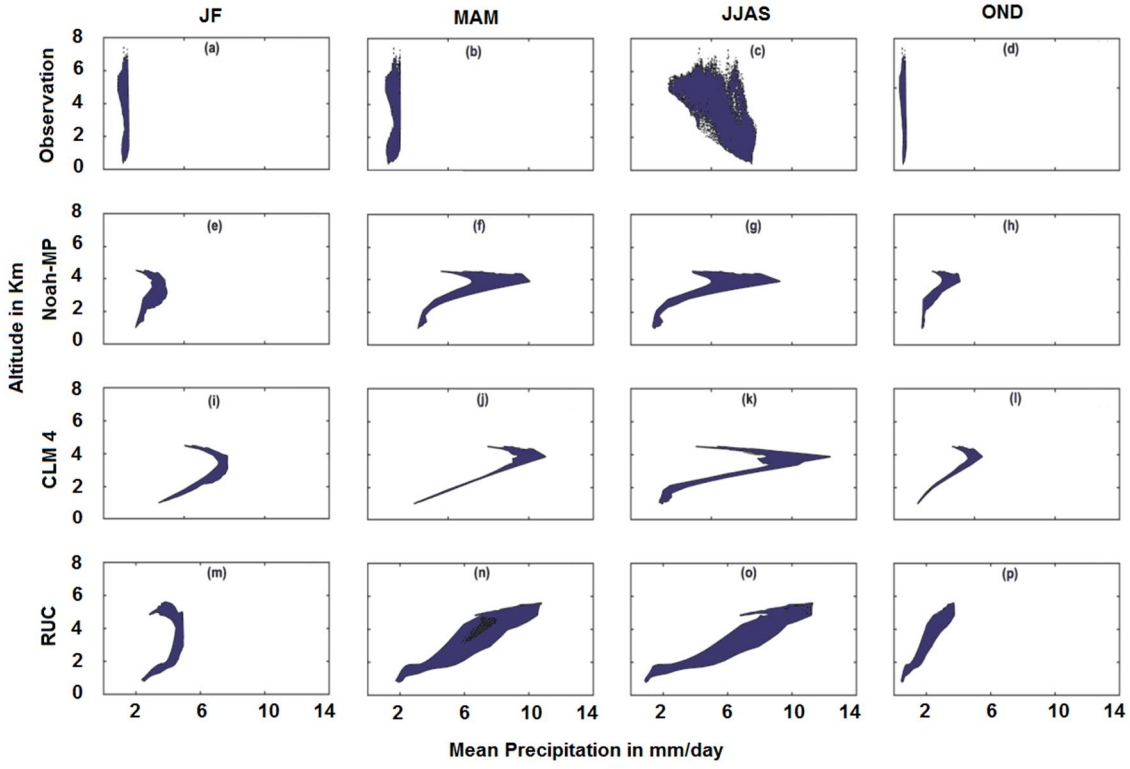

Figure 5. Distribution of precipitation with respect to elevation over the study area

IV. DISCUSSION

Considering that the orographic flow regime depends on the wind speed U, static stability N and mountain height h through the non-dimensional mountain height parameter (H = hN/U, Smith, 1979), which discriminates between "flow over" (H < 1) and "flow around" (H > 1), this results suggest that a true representation of one of all of these terms in the model simulations may be responsible for the accurate representation of the rainfall.

REFERENCES

[1] Ball, J. T., I. E. Woodrow, and J. A. Berry. (1987). A model predicting stomatal conductance and its contribution to the control of photosynthesis under different environmental conditions. Pages 221-224 in Proceedings of the 7th International Congress on Photosynthesis, Dordrecht, The Netherlands.
[2] Benjamin, S. G., , G. A. Grell, , J. M. Brown, , T. G. Smirnova, , and R. Bleck, (2004) Mesoscale weather prediction with the RUC hybrid isentropic–terrain-following coordinate model. Mon. Wea. Rev., 132 , 473–494.
[3] Berbery, E. H., , K. Mitchell, , S. Benjamin, , T. Smirnova, , H. Ritchie, , R. Hogue, , and E. Radeva, (1999) Assessment of land-surface energy budgets from regional and global models. J. Geophys. Res., 104, 19 329–19 348, doi:10.1029/1999JD900128.
[4] Bookhagen, B., and Burbank, D.W., (2010) Toward a complete Himalayan hydrological budget: spatiotemporal distribution of snowmelt and rainfall and their impact on river discharge J. Geophys. Res., 115, p. F03019 doi: 03010.01029/02009JF001426
[5] Dickinson, R. E., M. Shaikh, R. Bryant, and L. Graumlich (1998), Interactive canopies for a climate model, J. Clim., 11, 2823– 2836, doi:10.1175/1520-0442(1998)011<2823:ICFACM>2.0.CO;2
[6] Dickinson, R. E. (1983), Land surface processes and climate-surface albedos and energy balance, in Theory of Climate, Adv. Geophys., vol. 25, edited by B. Saltzman, pp. 305– 353, Academic, San Diego, Calif.
[7] Giorgi, F., Jones, C., & Asrar, G. (2009). Addressing climate information needs at the regional level: The CORDEX framework. WMO Bulletin, 58, 175– 183.
[8] Kaushik , S.D.(1962) . Climatic Zones and the Related Socio - economy of the Garhwal Himalaya . Geog . Rev. India , 24 (3-4)
[9] Nepal, S. and Shrestha, A.B. (2015) Impact of Climate Change on the Hydrological Regime of the Indus, Ganges and Brahmaputra River Basins: A Review of the Literature. International Journal of Water Resources Development, 31, 201-218.https://doi.org/10.1080/07900627.2015.1030494
[10] Niu, G.-Y., and et al. , (2011) The community Noah land surface model with multiparameterization options (Noah-MP): 1. Model description and evaluation with local-scale measurements. J. Geophys. Res., 116, D12109, https://doi.org/10.1029/2010JD015139.
[11] Niu, G.-Y., Z.-L. Yang, R. E. Dickinson, L. E. Gulden, H. Su, (2007), Development of a simple groundwater model for use in climate models and evaluation with Gravity Recovery and Climate Experiment data. J. Geophys. Res., 112, D07103, https://doi.org/10.1029/2006JD007522.
[12] Niu, G.-Y., and Z.-L. Yang, (2004) Effects of vegetation canopy processes on snow surface energy and mass balances. J. Geophys. Res., 109, D23111, https://doi.org/10.1029/2004JD004884.
[13] Oleson, K. W., et al. (2008), Improvements to the Community Land Model and their impact on the hydrological cycle, J. Geophys. Res., 113, G01021, doi:10.1029/2007JG000563
[14] Panday, P.K. J. Thibeault, K.E. Frey(2015)Changing temperature and precipitation extremes in the Hindu Kush-Himalayan region: an analysis of CMIP3 and CMIP5 simulations and projections,Int. J. Climatol., 35 (10) (2015), pp. 3058-3077
[15] Sati VP (2008) Natural resource management and food security in the Garhwal Himalaya. ENVISBull Himalayan Ecol 16(2):6–16
[16] Shukla, S.P., M.J. Puma, and B.I. Cook, 2014: The response of the South Asian Summer Monsoon circulation to intensified irrigation in global climate model simulations. Clim. Dyn., 42, no. 1-2, 21-36, doi:10.1007/s00382-013-1786-9.
[17] Skamarock, W. C., et al, (2008). A description of the Advanced Research WRF version 3. NCAR Tech. Note NCAR/TN-475+STR, 125 pp.
[18] Smirnova T.G., Brown J.M., Benkamin S.G., Kenyon J.S. (2016) Modifications to the Rapid update cycle land surface model (RUC LSM) available in the weather research and forecasting (WRF) model. Am. Meteorol. Soc. 2016;144:1851–1865.
[19] Smirnova, T. G., J. M. Brown, , and D. Kim, (2000) Parameterization of cold-season processes in the MAPS land-surface scheme. J. Geophys. Res., 105, 4077–4086, doi:10.1029/1999JD901047.
[20] Smith, R. B. (1979). The influence of mountains on the atmosphere. Adv. Geophys. 21, 87–230.
[21] Yang, Z.-L., and G.-Y. Niu (2003). The versatile integrator of surface and atmosphere processes (VISA) part I: Model description, Global Planet. Change, 38, 175– 189.
[22] Yatagai, A. Kamiguchi, K. Arakawa, O. et al. (2012). APHRODITE: Constructing a long-term daily gridded precipitation dataset for Asia based on a dense network of rain gauges,Bull. Am. Meteorol. Soc., 93 pp. 1401-1415
[23] A ting over Western and Central Himalaya by using Mesoscale Models" (International Journal of Earth and Atmospheric Science | July-September, 2014 | Vol 1 | Issue 2 | Pages 71-84)

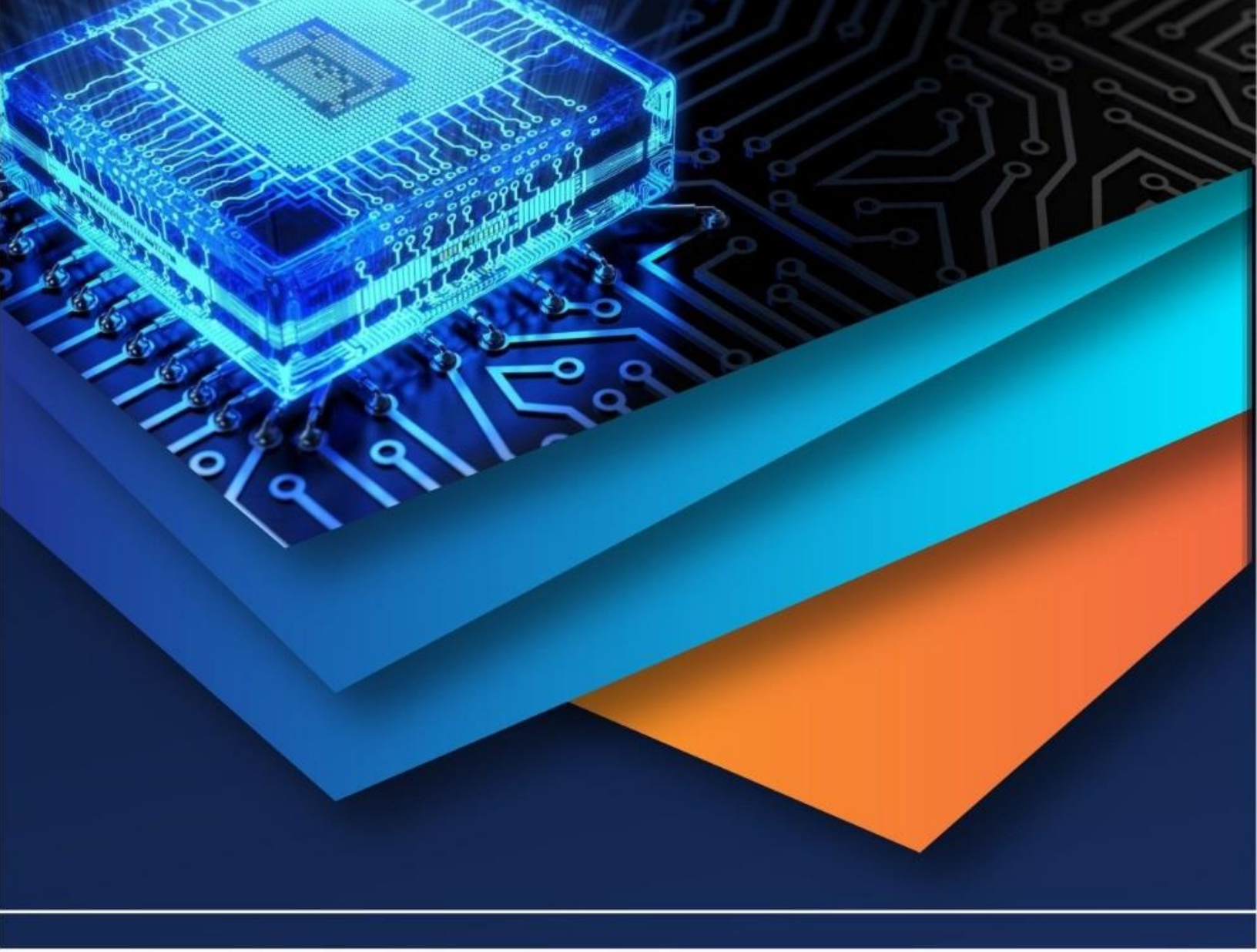

10.22214/IJRASET

45.98

IMPACT FACTOR: 7.129

IMPACT FACTOR: 7.429

INTERNATIONAL JOURNAL FOR RESEARCH

IN APPLIED SCIENCE & ENGINEERING TECHNOLOGY